






## Article

# Particle Deposition Pattern on an Automotive Diesel Filter Using an Eulerian Probability Density Function Method

Luis Valiño <sup>1</sup>, Radu Mustata <sup>1,\*</sup>, Juan Hierro <sup>2</sup>, Juan Luis Hernández <sup>3</sup>, María José García <sup>3</sup>, Carlos Blasco <sup>3</sup>, Yi-Tung Chen <sup>4</sup>, Lung-Wen Chen <sup>5</sup> and Prosun Roy <sup>4,5</sup>

<sup>1</sup> ICB/CSIC, María de Luna 10, E-50018 Zaragoza, Spain; l.valino@csic.es

<sup>2</sup> Centro Universitario de la Defensa, Carretera Huesca s/n, E-50090 Zaragoza, Spain; hierro@unizar.es

<sup>3</sup> Robert Bosch España Gasoline Systems, Raso de la Estrella, s/n, E-28300 Aranjuez, Spain; juanluis.hernandezcarabias@es.bosch.com (J.L.H.); mariajose.garciavargas@es.bosch.com (M.J.G.); carlos.blasco@es.bosch.com (C.B.)

<sup>4</sup> Department of Mechanical Engineering, University of Nevada Las Vegas, 4505 S Maryland Pkwy, Las Vegas, NV 89154, USA; yitung.chen@unlv.edu (Y.-T.C.); royp3@unlv.nevada.edu (P.R.)

<sup>5</sup> Department of Environmental and Occupational Health, University of Nevada Las Vegas, Harry Reid Center (HRC) for Environmental Studies, 4505 S Maryland Pkwy, Las Vegas, NV 89154, USA; antony.chen@unlv.edu

\* Correspondence: radu.mustata@csic.es

**Abstract:** A full 3D numerical simulation of the two-phase flow made up of (bio)diesel and particles, has been carried out to reproduce the deposition pattern of particles in a BOSCH automotive filter. From a probability density function (PDF), a simple Eulerian-Eulerian two-phase model is proposed for diesel and particles. The proposed formulation allows for a detailed description of the relationship between the velocity and size of the particles. A Brinkman-Darcy approximation has been considered for the flow through the filtering paper and is proved to be sufficient for the typical filter working conditions. The new tool is able to reproduce the deposition pattern shown by the used filters.

**Keywords:** filter; two-phase flows; Eulerian probability density function; particle size distribution



**Citation:** Valiño, L.; Mustata, R.; Hierro, J.; Hernández, J.L.; García, M.J.; Blasco C.; Chen, Y.-T.; Chen, L.-W.; Roy, P. Particle Deposition Pattern on an Automotive Diesel Filter Using an Eulerian Probability Density Function Method. *Processes* **2023**, *11*, 1100. <https://doi.org/10.3390/pr11041100>

Academic Editors: Omar Dario Lopez Mejia and Santiago Lain

Received: 8 March 2023

Revised: 27 March 2023

Accepted: 29 March 2023

Published: 4 April 2023



**Copyright:** © 2023 by the authors. Licensee MDPI, Basel, Switzerland. This article is an open access article distributed under the terms and conditions of the Creative Commons Attribution (CC BY) license (<https://creativecommons.org/licenses/by/4.0/>).

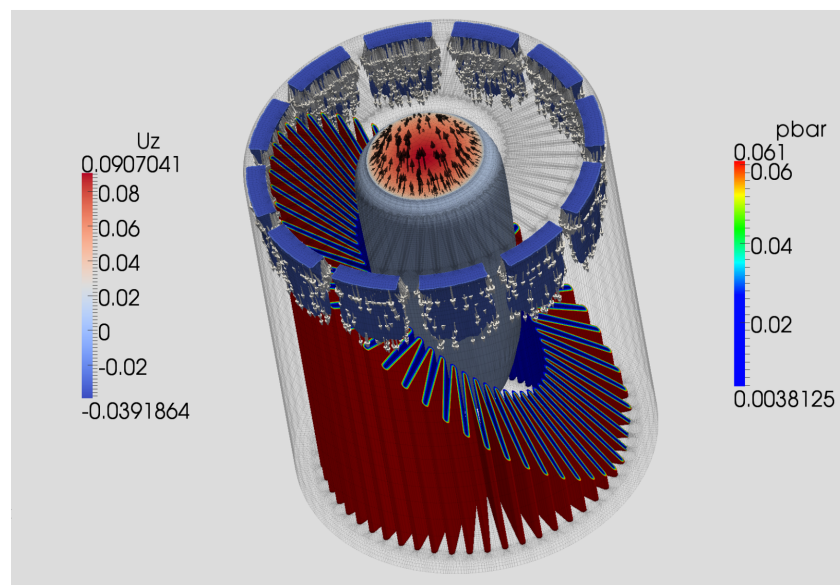
## 1. Introduction

The “trial and error” method is still the usual way to design new filters. This method is both time- and cost-consuming, as it implies the design and construction of various experimental test grids and prototypes that render the process difficult or impossible to systematize [1]. At the most basic level, filtration is the process of separation from a fluid suspension of undesired (or desired) particles while passing through a porous medium (the filtering medium). The filter design can vary widely depending on the application, in terms of both the internal pore structure (microscale design) and how the filtering medium is deployed (macroscale design). However, not just any simple design can be deemed fit for this purpose. The challenge for the automotive industry is not only to design filters with higher efficiency but also, with the ever-increasing limits in space, to design filters with smaller physical sizes. The most common design used to achieve this tradeoff is the single-pass pleated filtering media approach (see Figure 1a); such a design is subject to study in this present paper.

In the automotive industry, computational fluid dynamics (CFD) simulation programs are already an established tool in the R&D departments, aimed at reducing the development and time costs of designing different vehicle parts, such as injectors, inlet and outlet manifold design, exhaust systems, etc. Although these tools have been used for more than 20 years in the automotive world, CFD programs are still not standard tools for fuel filter development. The first numerical tools have been created only recently, with the lack of both appropriate models and algorithms being the factors behind this delay [2,3]. In order to reduce prototyping cycles, it is convenient to have a specific numerical simulation tool on hand that can model particle filtration during the design stage.



(a)



(b)

**Figure 1.** (a) Bosch filter device with the external holder removed to see the filtering medium. The flow enters vertically through the upper-side external slots and exits through the upper-side central duct; (b) 3.3 M cell mesh with pressure drop and velocity pattern.

Modern injection systems are very sensitive to the possible presence of solid particles in the fuel (diesel or gasoline) since these particles can damage the injectors due to corrosion, abrasion, or other effects [4]. Therefore, it is necessary to guarantee a certain level of particle cleanliness to ensure that injection systems work properly throughout the entire operating lifetime.

Diesel fuels contain a higher amount of water than gasoline (up to 500 ppm). In the case of biodiesel, this is even worse. Consequently, it is necessary to filtrate an extra amount of water [5] since water can cause corrosion problems in the injectors. Fuel filters for diesel engines have to be able to filtrate the particles contained in the fuel and separate the water droplets, which normally are collected at the bottom of the filter and purged periodically.

In diesel filtering, the considered flow is made up of a liquid for the continuous phase and a solid for the discrete phase. Other relevant situations in particle filtering

in the automotive industry involve gas-solid combinations, such as in the exhaust gas manifold [6].

Filtering media must provide a certain level of efficiency depending on customer requirements and/or particular industrial standards. In addition, the filter must have a specific particle retention capacity. This capacity is defined by means of a change interval or lifetime, which represents the guaranteed amount of kilometers before the filter gets clogged due to the retained particles and has to be changed.

The use of either a filter with a wrong design or a filter medium that leads to lower particle efficiency or a shorter lifetime, may have negative consequences, such as injector damage or filter clogging. Therefore, the engine system must include a fuel filter, especially for diesel engines, whose fuel contains a higher amount of particles.

From the numerical point of view, the simulation of multi-phase flows is not only an interesting scientific challenge but, due to the number of industrial applications, such as chemical reactors, combustion devices, medical inhalers, etc, it is also motivated by economical and safety considerations. In the study of the single-pass filters for (bio)diesel-from now on, diesel-vehicles, the difficulty is enhanced due to the presence of the fluid flow through a porous medium coupled with the interaction between the filtering medium and the particles. On the other hand, the flow rates in normal operating conditions render small Reynolds numbers, i.e., laminar flow conditions. In any case, once the models have been established, a code is needed to adequately discretize such models in the flow domain and to numerically solve the resulting linear equations.

This paper presents one new CFD approach to solve the flow in a diesel filter device, with the initial application to numerically reproduce the deposition pattern of particles shown on a filter under real conditions. The paper is structured in various sections. In Section 1, a brief description of an automotive diesel filter in a general situation is given. In Section 2, a model is presented for the two-phase flow composed of diesel and particles, based on a probability density function (PDF) approach [7] for the diluted phase position and size. In Section 3, the Brinkman-Darcy approximation for the flow through the filtering paper [8] is shown to be adequate for normal operating conditions of diesel filters. In Section 4, the numerical results are depicted, which show a very good qualitative agreement in terms of the deposition of particles on a used filter. Conclusions are drawn, and future work is suggested.

## 2. Eulerian-Eulerian Statistical Approach

In this section, the modeling approach of (solid) particles in a diesel flow is explained. Water filtering has a different behavior and will be the subject of another study.

There are several alternatives for predicting the evolution of two-phase flows, depending on the approximation used to solve each phase. In Eulerian-Lagrangian approaches, the continuous phase (diesel, in our case) is solved in the usual Eulerian frame. The dispersed phase elements (solid particles, in our case) are tracked throughout the simulation, and their interactions with the continuous phase are taken into account locally. These methods, such as the Discrete Phase Model [9], are known to be able to reproduce accurately the behavior of the system, but they can be numerically expensive, as a large number of discrete elements must be used. Moreover, a mixed Lagrangian-Eulerian code is needed.

In Eulerian-Eulerian approaches, both phases are treated as being continuous after introducing some kind of averaging procedure (time, space, ensemble, etc.) in the discrete phase. The exact knowledge of the position of the particles is lost, which is, in principle, a disadvantage for the modeling of the interaction between both phases, although, depending on the averaging procedure, the necessary information for local interaction may be kept (as in the present paper). As the formulation is purely Eulerian, the usual discretization and numerical algorithms can be used in opposition to Eulerian-Lagrangian formulations.

In the present paper, an Eulerian-Eulerian approach is used. To choose the most convenient average of the discrete phase, an analysis of the relevant interaction phenomena in the present problem is pertinent. The void fraction of particles (the fraction of the total volume occupied by particles) is extremely small. That means that both the particle-particle

interaction and the influence of the particles on the diesel can be neglected. Therefore, the flow of diesel can be solved independently. In the present case, the flow is laminar (the Reynolds number is well below 200 in all cases), so there is no need for any turbulence modeling, although other difficulties arise, as shown in Section 3.

On the other hand, the effect of the fluid on the particles should be considered, along with the gravity field. The key parameter is the particle size since the forces acting on the particles are directly related to their size. At this point, it should be stated that only spherical particles are to be considered in this study. Of the various forces that can act on the particles, such as drag, history (Basset), and buoyancy, the drag is considered the most relevant under the present highly diluted conditions. The effect of gravity/buoyancy may also be important for the bigger particles, given the density difference between the fluid and the particles, so it should be taken into account as well. As the density of the particles used to verify the filter quality is constant, the buoyancy is proportional to the cube of the radius. In the end, the particle radii and velocities are the only relevant magnitudes needed to characterize their evolution.

With these simplifying assumptions, the transport equations of the magnitudes characterizing the discrete phase as a function of the particle radius may be obtained. In strictly obtaining this, a probabilistic description should be considered. The reason is that boundary conditions for the particles are only known in a probabilistic sense. One knows that the particles entering the filter follow a specified size distribution, but no information about the specific position, velocity, or size of any single particle in the flow is available. Even this statistical information about the discrete phase at the boundaries is rather incomplete, although some plausible assumptions make this limited information sufficient. The details are found in Appendix A.

The resulting transport equations are, however, quite intuitive; firstly, we have a continuity-like equation to express the conservation of the number density for the particles of each radius (there is no agglomeration or wear of the particles):

$$\frac{\partial n(r, \mathbf{x}; t)}{\partial t} = - \frac{\partial}{\partial x_j} \left[ u_j^p(r, \mathbf{x}; t) n(r, \mathbf{x}; t) \right] \quad (1)$$

where  $n(r, \mathbf{x}; t)$  is the expected number density of particles of the size  $r$  at position  $\mathbf{x}$ , and  $\mathbf{u}^p(r, \mathbf{x}; t)$  is their corresponding velocity. Secondly, the momentum conservation adopts the form of the evolution of the velocity of small spherical particles in a laminar flow, considering only the dominant terms, drag, and buoyancy in our case [10]:

$$\begin{aligned} (\rho^p + 0.5\rho) \frac{4\pi r^3}{3} \frac{du_i^p}{dt} &= (\rho - \rho^p) \frac{4\pi r^3}{3} g_i \\ &\quad - 3\rho\pi r v (u_i^p - u_i) \\ &\quad - \frac{9\rho\pi r^2}{4} \|u_i^p - u_i\| (u_i^p - u_i) \end{aligned} \quad (2)$$

where  $\rho^p$  and  $\rho$  are the densities of the particles and the fluid, respectively;  $4\pi r^3/3$  is the volume of a spherical particle with diameter  $r$ ;  $v$  is the kinematic viscosity;  $\mathbf{u}$  is the fluid velocity; and  $d/dt$  stands for the total time derivative of the velocity of the particle, that is to say, its total acceleration or its Lagrangian time derivative. In Equation (2), the left term represents the linear momentum variation of a spherical particle and its added mass (because of the equivalent volume of fluid, which moves with the particle), whereas, on the right side, there is first a buoyancy contribution and, next, a drag contribution up to the second order to the relative velocities (the velocity of the particle relative to that of the fluid) with an approximation valid for those velocity particles whose Reynolds number, based on the relative velocity, is less than one, or the theoretical observed drag.

Values for the fluid properties and particle sizes are taken from those of Shell Fluid 41 doped with the fine test dust A2 ISO 12103-1. The details are shown in Table 1.

**Table 1.** Flow properties and geometrical data. The intake area is the area of the annulus of the filter, taking out the small section of the internal separating walls. Filtering paper K11B40A. Fluid values for Shell Fluid 41. Fine test dust A2 ISO 12103-1 approximated by a Weibull distribution.

Geometrical	Inflow area	9.13 cm <sup>2</sup>
	Filter height	89.7 mm
	Outer annulus diameter	80 mm
	Inner annulus diameter	70 mm
	Exit duct diameter	25 mm
Filtering Media	Permeability $K$	$2.81 \times 10^{-13}$
	Porosity $\varepsilon$	0.517
	Paper thickness $L$	0.65 mm
Flow	Flow rate	120 L/h
	Fluid density	850 kg/m <sup>3</sup>
	Fluid kinematic viscosity	13.6 cSt
	Particle density	2650 kg/m <sup>3</sup>
	Dust concentration	50 mg/L
	Prob. density function	$\beta \frac{x^{(\beta-1)}}{xref^\beta} e^{-\left(\frac{x}{xref}\right)^\beta}$
	Size parameter	$xref = 14.3 \mu\text{m}$
	Shape parameter	$\beta = 1.1$

The boundary conditions at the inlet are given by the expected density number for each particle size following a prescribed Weibull probability density function for the A2 dust, which is equally distributed in space and with particles that match the fluid velocity at the domain entry. At the exit, zero gradient conditions are used, while non-slip conditions are prescribed at walls. Notice that the void fraction information is known from  $n(r, \mathbf{x}; t)$ .

### 3. Diesel in the Paper Filter: Darcy-Brinkman Approximation

From the diesel point of view, as the flow inside the filter is not affected by the particles during this short time (the permeability evolves very slowly in comparison to the flow characteristic time), a single-phase flow in a porous medium is to be studied. This is the object of the present section.

We use the approximations of Ochoa-Tapia and Whitaker [11] as the most convenient way to describe the flow in the free and porous medium:

$$\frac{\partial u_i}{\partial t} + \frac{\partial u_i u_j}{\partial x_j} = -\frac{1}{\rho} \frac{\partial P}{\partial x_i} + \frac{\partial}{\partial x_k} \left( \nu \frac{\partial u_i}{\partial x_k} \right) \quad (3)$$

$$\frac{1}{\varepsilon} \frac{\partial u_i}{\partial t} + \frac{1}{\varepsilon^2} \frac{\partial u_i u_j}{\partial x_j} = -\frac{1}{\rho} \frac{\partial P}{\partial x_i} + \frac{\partial}{\partial x_k} \left( \frac{\nu}{\varepsilon} \frac{\partial u_i}{\partial x_k} \right) - \frac{\nu}{K} u_i, \quad (4)$$

where  $P$  is the fluid pressure without the hydrostatic contribution,  $\varepsilon$  is the porosity (the empty volume fraction available for the fluid), and  $K$  is Darcy's permeability in units of  $[L]^2$ . The flow is assumed to be incompressible and to have a constant density; that is to say, the null divergence constraint is applied on the velocity field,  $\nabla \cdot \mathbf{u} = u_{i,i} = 0$ . The gravitational effects on the fluid may be considered canceled with the hydrostatic pressure gradient.

In Equation (4), the velocity is really a superficial volume average,

$$u_i \equiv \langle u_i \rangle_S = \frac{1}{V} \int_V u_i dV = \varepsilon \frac{1}{V_{free}} \int_V u_i dV = \varepsilon \langle u_i \rangle_I, \quad (5)$$

whereas the pressure is an intrinsic volume average.

$$p \equiv \langle p \rangle_I = \frac{1}{V_{free}} \int_V p dV = \frac{1}{\varepsilon} \frac{1}{V} \int_V p dV = \frac{1}{\varepsilon} \langle p \rangle_S. \quad (6)$$

These two types of averages, related by the porosity  $\varepsilon$ , are chosen because they match the velocity and pressure variables, respectively, from Equation (3) at the interface [11]. For this reason, no average operator is written explicitly in the paper.

It should be noted that in Equation (4), one could add a second-order term, the Forchheimer correction, to its right side, as follows: [12]

$$-\frac{F}{K^{1/2}}(u_j u_j)^{1/2} u_i \quad (7)$$

where  $F$  is a non-dimensional coefficient. However, the usual velocity magnitudes present in the filtering problem with which we are dealing are small enough, and this leads to neglect of Forchheimer's correction from the formulation. One should also be aware that the permeability is, in general, a second-order tensor, so  $K^{-1}u_i$  should really be  $K_{ij}^{-1}u_j$ . Again, the filtering paper is assumed to be isotropic at least along its flow-normal direction; that is to say,  $K_{ij}^{-1}u_j = K^{-1}u_n$ , and the work can be performed with a scalar permeability.

Averages are computed over a mesoscopic (larger than the pore size, smaller than the large-scale variations of the fluid) porous zone. In this sense, the previous equations should be understood as valid on that scale.

The fluid and porous zones may be integrated as two different domains using Equations (3) and (4), respectively, plus the incompressibility constraint, which is linked by a proper boundary condition [13] as follows:

$$\begin{aligned} \mathbf{u}_f &= \mathbf{u}_p \\ P_f &= P_p \\ v \frac{\partial \mathbf{u}_f}{\partial x_i} n_i &= \frac{v}{\varepsilon} \frac{\partial \mathbf{u}_p}{\partial x_i} n_i \end{aligned} \quad (8)$$

where  $\mathbf{n}$  represents the vector normal to the fluid-porous interface, and the sub-indexes  $f$  and  $p$  stand for the fluid and porous media at the interface, respectively.

There is also the possibility of modeling the coupling between the porous and fluid media by assuming that the whole computational domain represents a heterogeneous fictitious porous medium [14] where  $\varepsilon = 1$  and  $k = \infty$  in the free zones. This approach is justified [14] at least in the Stokes case (without advection). Equation (4) is applied in the full domain with the incompressibility constraint [15] and variable values of  $\varepsilon$  and  $K$ , with a gradient singularity at the inner interface between the porous and fluid media. That is the approach followed in the present paper.

#### 4. Numerical Results

Due to the purely Eulerian approximation applied, the two-phase formulation proposed here has been incorporated into a standard CFD solver, OpenFOAM. OpenFOAM [16] is a software package that solves partial differential equations discretized on 3D unstructured meshes by finite volume methods. It is open-source, so the code can be modified to the needs of each particular problem. Usually, some of the available pre-configured solvers are used as a template and adapted, as in the present filtering problem. A computational fluid dynamics SIMPLE algorithm was appropriate for the present case.

To represent the porous filter, a specific permeability value has been chosen by fitting the pressure drop of a clean filter. This means that a snapshot of the behavior of the filter at a particular time has been used. In fact, a different value does not change the general pattern of the flow of particles, whose study is the main objective of this paper.

A typical filtering element without clogging is depicted in Figure 1a. The numerical results for the pressure drop through the filter and the vertical component of the flow velocity are presented in Figure 1b. An optimized all-hex 3.3 M cell mesh is used for this purpose. A mesh detail from a cut through the filtering media is presented in Figure 2a whilst the flow through the filtering media is detailed in Figure 2b. The mesh in the normal direction of the interface(s) (free media (blue wireframe)/porous media (green/pink

wireframes)) has been kept at a comparable size on either side of the interface(s). A WENO-like approach for pressure/velocity has been used in the treatment of the interface to avoid the under- and overshoots in the velocity profile.

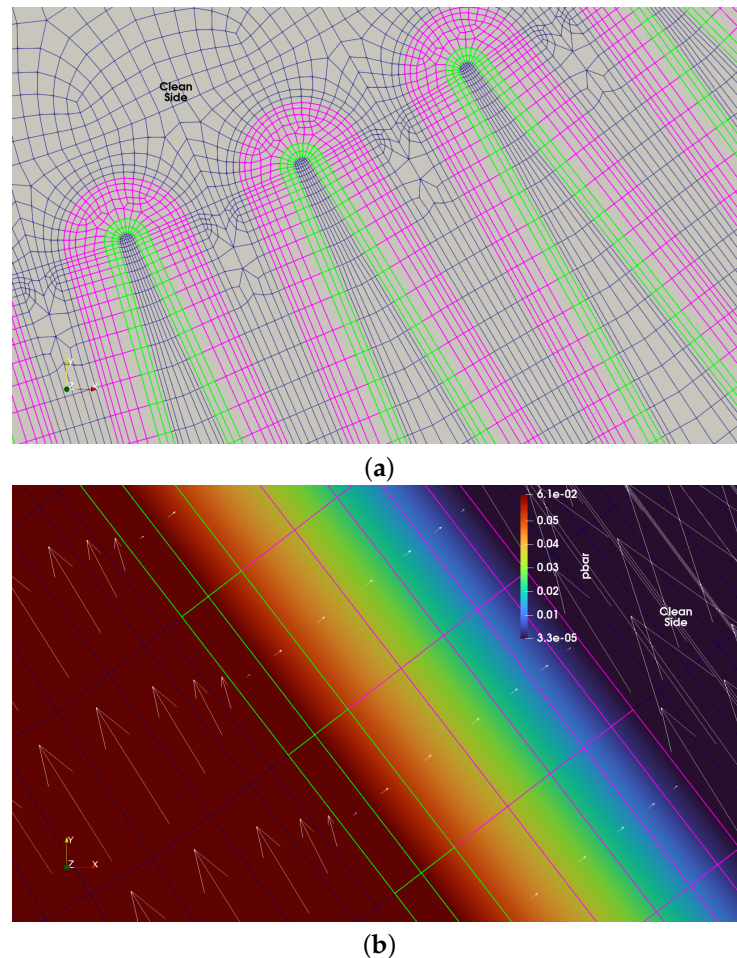


**Figure 2.** (a) Mesh detail in a plane through the filtering device (normal to z-direction); (b) velocity vectors and pressure drop detail through the same plane.

As can be observed in Figures 1b and 2b, most of the pressure drop takes place in the filtering media. The two-layer composition of the filtering media, the hydrophobic (melt-blown), and the cellulose are highlighted in Figure 2b with green and pink wireframes, respectively. However, for the performed 3D numerical simulation, both media were assigned the same properties (permeability and porosity), as given in Table 1. The computational domain was reduced to a sixth of the full filtering device by taking into account its cylindrical symmetry, as depicted in Figure 3, thus enabling reasonable computing times to be achieved (under two hours CPU time on an Intel Core i7-7700K four cores 4.2 GHz).

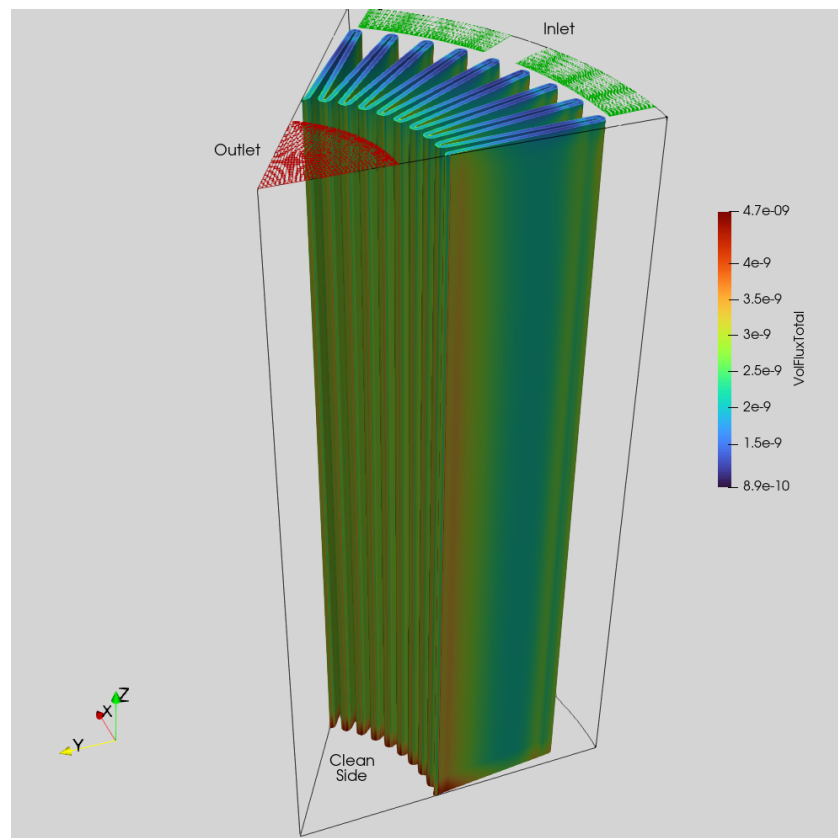


**Figure 3.** Flux of particle mass arriving at the filtering media.

It is worth pointing out that horizontal velocities tend to become normal across the filter medium, whilst, inside the free medium, they tend to align with the porous-free interface, as can be seen in Figure 2b. This effect is a natural, expected consequence of the presence of a Darcy medium (the filter) with low permeability. High lateral pressure gradients parallel to the porous-free medium interface would imply (see Equation (3)) high fluid accelerations and high velocities inside the free medium, which, in turn, would render the flow incompatible with mass conservation and the provided boundary conditions. As a result, most of the pressure drop inside the porous medium must be normal to those interfaces. With the typical values of permeability in the studied filter, the dominant contributions to the flow inside the porous medium (see Equation (4)) are the pressure gradient and the Darcy one, which cancel each other almost exactly. With regard to the free medium, the presence of a porous-free interface acts as a barrier that leads the flow to try to surround it, until it impinges upon the inner corners of the filter folds. Of course, there is a certain amount of flow passing through the filter before the folds as can be seen in Figure 2b.

In Figure 3, the total mass per unit area and the arrival time at the clean filter are shown. The qualitative agreement with Figure 4 is obvious, and the pattern is well explained using the same considerations as in the previous paragraph: the porous-free interface leads most of the incoming flow towards the folds of the filter through which, subsequently, more particles are going. Eventually, and in longer calculations than those reported in this paper, the flow would be diverted from the folds and become more evenly distributed along the filter: particle deposition starts at the inner side of the folds and propagates upstream from there (see Figure 4).



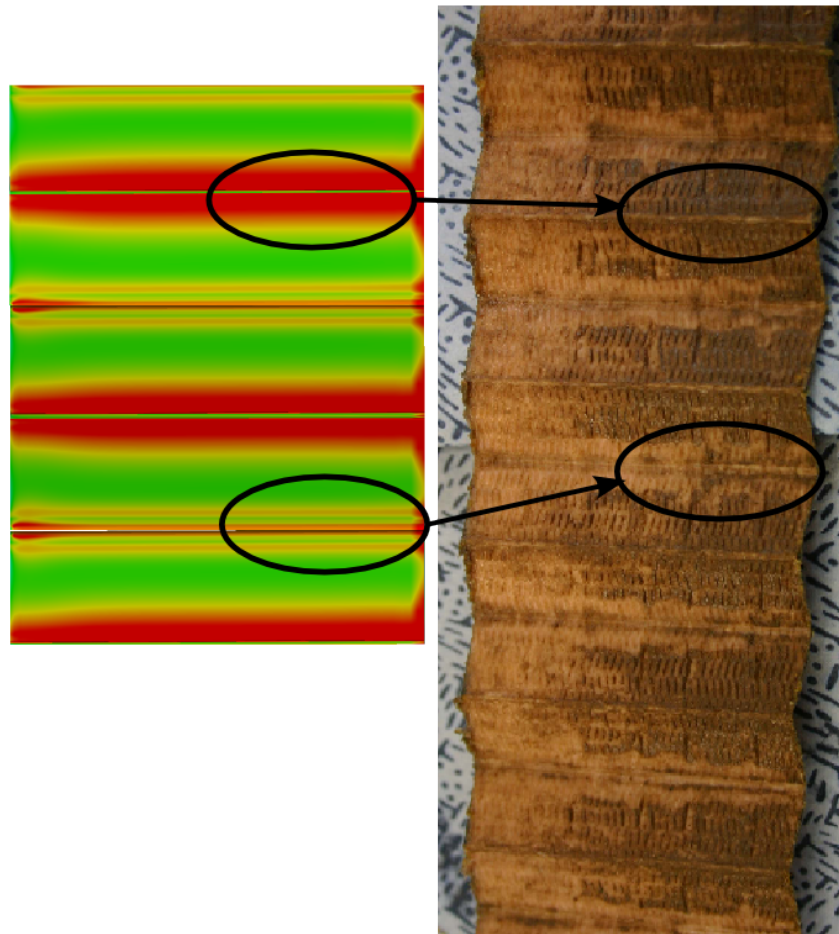


**Figure 4.** Unfolded view of a typical stained filter and comparison with numerical results.

It should be noticed that the real conditions are not known. This includes, among other things, the type of diesel used, its cleanliness, its particle distribution, its vibrations, etc. Those effects should distort somehow the deposition pattern, which is preserved, nevertheless, in its general characteristics. This is so that the main features of the flow, described above, are not fundamentally affected by those effects.

In Figures 5–7, the same quantity, or the particle number flow through a clean filter, is depicted but for progressively larger sized particles. One can notice the increase in gravitational effects as the particles grow in size. This effect may be noticed in Figure 4, and, in the total mass simulation, Figures 3 and 7, as well; there is not only a tendency for particles to accumulate starting from the folds but also from its bottom area where the larger sized particles aggregate. The most interesting feature of these simulations is that both these cited effects may be explainable without resorting to long calculations with variable permeability. In a clean filter with uniform properties, the flow is diverted so as to increase the flow of filtered particles through the areas that, eventually, would become more clogged.

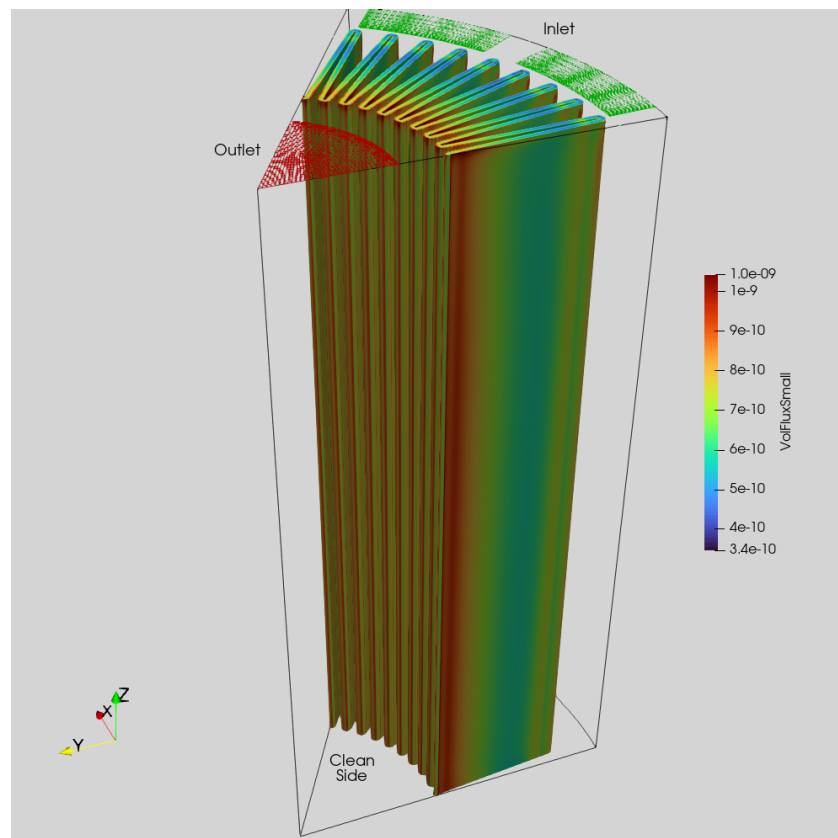


**Figure 5.** Flux of particle mass for particles with diameters of less than 10 μm.

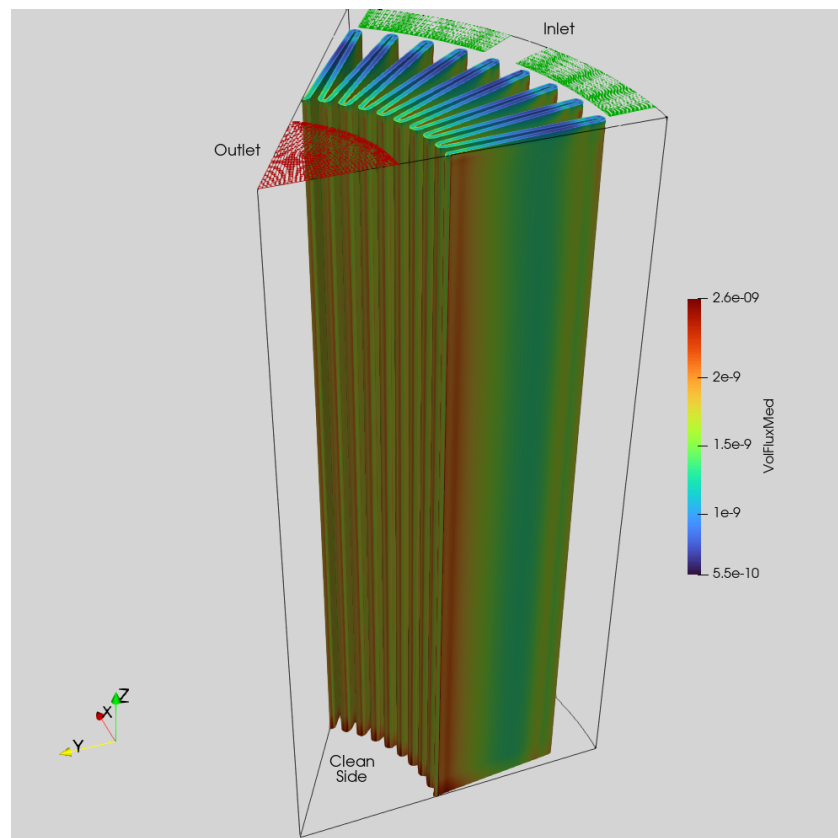


**Figure 6.** Flux of particle mass for particles with medium-sized diameter ( $30 \leq d \leq 40 \mu\text{m}$ ).

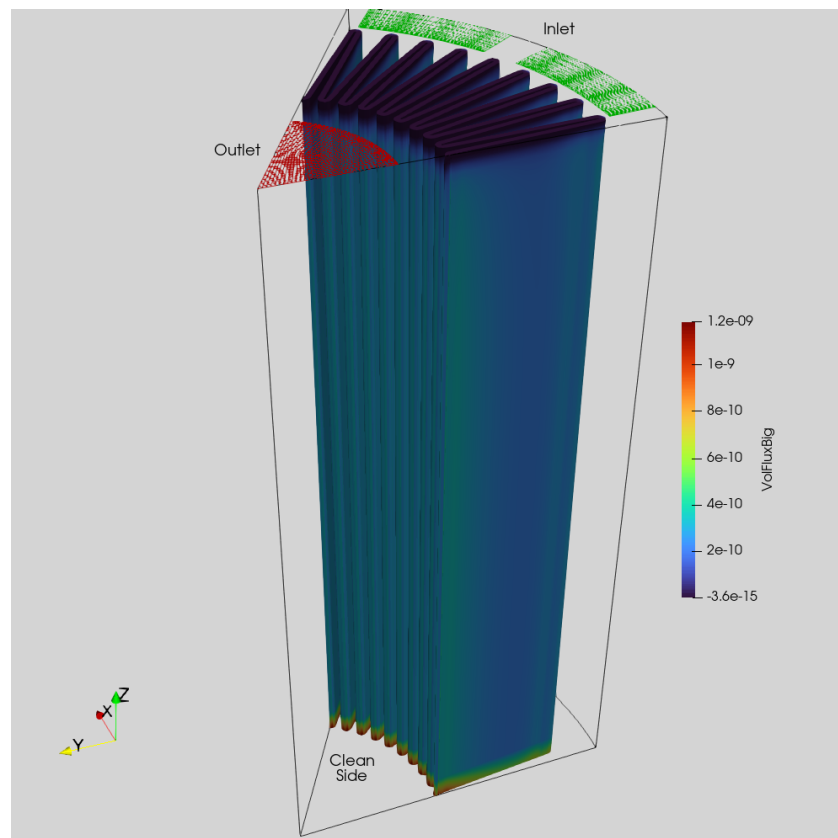


**Figure 7.** Flux of particle mass for particles with diameters in the upper range of the distribution ( $\geq 70 \mu\text{m}$ ).

#### *Quantitative Comparisons*

Although some small-scale distribution measurements are available [17], there are no experiments to date that provide measurements of the spatial distribution of the mass of particles absorbed in filters, such as the one studied in this article. In order to quantify the good qualitative agreement observed between the flow pattern computed through a clean filter and its observed amount of particle deposition, one further step has been considered, and the findings are presented in Figure 8. As long as clogging does not significantly affect the filter properties, the spatial distribution of the mass absorption will essentially remain unchanged; only the local values will increase proportionally with time. Therefore, if we normalize by the maximum value, the distribution is independent of time. It is recalled that this is valid for relatively early times in the life of the filter, that is to say, as long as the effect of clogging can be neglected.

For the filter, the picture (Figure 4 or Figure 8a) has been taken with a camera with a linear response, and it is assumed that there is also a linear relationship between the gray intensity level and the absorbed mass. This last assumption will be revisited later in this section. In addition, a linear relationship is established between the numerical results and the gray level of their representation (the grayscale version of the left side of Figure 4). The gray levels are normalized in the  $[0, 1]$  range, with 1 representing the clearest value and 0 the most opaque one.

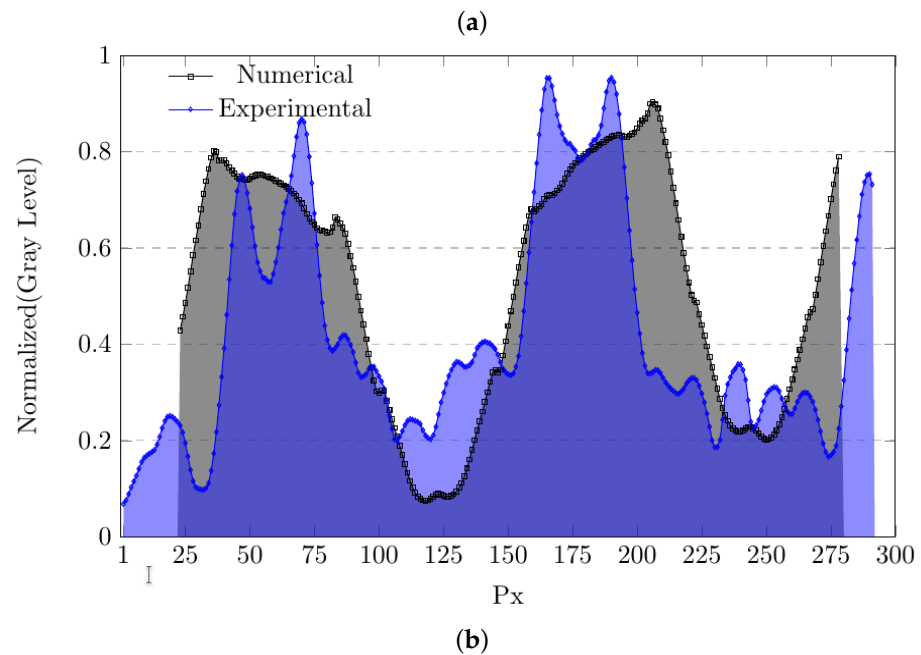
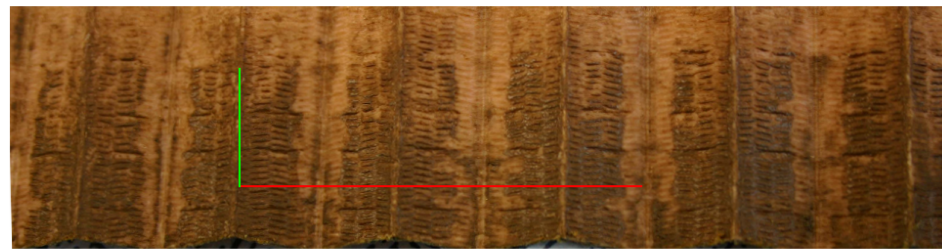


**Figure 8.** Intensity profile: (a) averaging zone; (b) comparison. Notice the effect of the pleats that are in contact with the upper side of the real device, which yields a double-peaked profile.

Due to the inherent noisiness of the data, and in order to perform a valid comparative analysis, one has to perform some kind of spatial averaging. A representative area determined by the red and green lines of Figure 8a and its counterpart of the numerical data have been considered for a two-step averaging procedure, resulting in the intensity data profiles represented in Figure 8b. Firstly, the intensity profile was extracted by sweeping across the red line and averaging along the green line. Secondly, the moving averages of a size (15 px), which preserves the main features of the profiles, are calculated over the intensity data obtained in the first step. The experimental irregularities in the pattern for the higher and lower peaks of the profile reflect the impossibility of having perfect pleats without deformations or any contact between their inner sides. The percentage difference between the integrated values of the two curves (shaded areas in Figure 8b), which represent the total mass of particles absorbed by the filtering area considered, amounts to 8.43%. This relatively small difference is consistent with the assumption of the linearity that exists between the gray level and the absorbed mass.

## 5. Conclusions

The full 3D simulations of particle filtering inside an automotive filter have been presented, in which the continuous phase governing the equations is supplemented with transport equations for the particle size distribution. The deposition pattern of particles on a BOSCH filter used under real conditions has been qualitatively reproduced with good quantitative behavior during the initial phases of clogging. This shows the potential of this tool. In future work, a model relating pressure drop with particle clogging should be

developed in order to estimate the evolution of permeability and predict the lifetime of the filtering element.

**Author Contributions:** Conceptualization, L.V., R.M., J.H., J.L.H., M.J.G., C.B., Y.-T.C., L.-W.C. and P.R.; methodology, L.V., R.M. and J.H.; software, L.V., R.M., J.H. and P.R.; validation, L.V., R.M., J.H., J.L.H., M.J.G. and C.B.; formal analysis, L.V., R.M., J.H., Y.-T.C., L.-W.C. and P.R.; investigation, L.V., R.M., J.H. and P.R.; resources, L.V., R.M., J.H., J.L.H., M.J.G. and C.B.; data curation, L.V., R.M., J.H. and P.R.; writing—original draft preparation, L.V., R.M., J.H. and J.L.H.; writing—review and editing, L.V., R.M., J.H., Y.-T.C., L.-W.C. and P.R.; visualization, L.V., R.M. and J.H.; supervision, L.V.; project administration, L.V. and R.M.; funding acquisition, L.V. and C.B. All authors have read and agreed to the published version of the manuscript.

**Funding:** This work was partially funded by the Spanish Government through the CENIT PIIBE project and the CSIC Intramural Grant 202260I190.

**Data Availability Statement:** Data sharing is not applicable to this article.

**Conflicts of Interest:** The authors declare no conflict of interest. The funders had no role in the design of this study; in the collection, analyses, or interpretation of data; in the writing of the manuscript; or in the decision to publish the results.

## Appendix A

For a statistical description of the discrete phase, in which the particles are moving in the diesel, the appropriate quantity is the droplet density function first introduced to describe the droplets' evolution in a spray [18,19]. The droplet density function  $n(\mathbf{v}, r, \mathbf{x}; t)$  is defined such that

$$n(\mathbf{v}, r, \mathbf{x}; t) d\mathbf{v} dr d\mathbf{x}$$

is the expected number of particles with velocities in the interval  $(\mathbf{v}, \mathbf{v} + d\mathbf{v})$ , radii in the interval  $(r, r + dr)$ , and positions in the interval  $(\mathbf{x}, \mathbf{x} + d\mathbf{x})$ . This function contains all the statistical information needed to describe our system.

Using conditional statistics, we can express this function as

$$n(\mathbf{v}, r, \mathbf{x}; t) = n(r, \mathbf{x}; t) P(\mathbf{v}|r, \mathbf{x}; t), \quad (\text{A1})$$

where  $n(r, \mathbf{x}; t)$  is the expected number density of particles with the radius  $r$  and position  $\mathbf{x}$  at time  $t$ , and  $P(\mathbf{v}|r, \mathbf{x}; t)$  is the probability density function (PDF) of the particle velocity, conditional on the radius  $r$  and position  $\mathbf{x}$  at time  $t$ . For the present analysis, we will derive transport equations for the two quantities on the right-hand side of Equation (A1) to obtain the statistical information of the discrete phase.

First, the expected number density  $n(r, \mathbf{x}; t)$  is analyzed. This is the probable density of the particles found in the small region  $d\mathbf{x} dr$ . It can be easily expressed by means of the Lagrangian PDF  $P_{\mathbf{x}^{\text{p}^+} r^+}(\mathbf{x}, r; t)$  of the particle radius  $r^+$  and position  $\mathbf{x}^{\text{p}^+}$  (where the sign  $+$  is used to indicate the Lagrangian frame) [20]:

$$P_{\mathbf{x}^{\text{p}^+} r^+}(\mathbf{x}, r; t) = \frac{n(\mathbf{x}, r, t)}{N}, \quad (\text{A2})$$

where  $N$  is the total number of particles in the domain, which is supposed to have negligible fluctuations. Integration of the number density  $n$  over a finite region in  $(\mathbf{x}, r)$  space would then provide the probable number of particles in that region.

Remember that the statistical information of  $n(r, \mathbf{x}; t)$  is equivalent to that provided by  $P(\mathbf{x}, r; t)$  once the total number of particles is known. As  $N$  should be a piece of provided information, next, a transport equation will be derived for  $P(\mathbf{x}, r; t)$ .

From the theoretical point of view, the description based on this PDF comes from a description of an ensemble average (the average of a set of identical systems). Its transport equation can be derived by standard methods [20]:

$$\begin{aligned} \frac{\partial P(r, \mathbf{x}; t)}{\partial t} = & -\frac{\partial}{\partial x_j} \left[ \overline{\left( \frac{dx_j^+}{dt} \middle| \mathbf{x}, r \right)} P(r, \mathbf{x}; t) \right] \\ & -\frac{\partial}{\partial r} \left[ \overline{\left( \frac{dr^+}{dt} \middle| \mathbf{x}, r \right)} P(r, \mathbf{x}; t) \right] \\ & -JP(r, \mathbf{x}; t) \end{aligned} \quad (\text{A3})$$

where the overline represents an ensemble averaging, and the terms inside the parentheses are conditional-averaged quantities (in the ensemble average approximation).  $J$  is the net flux of the probability of the PDF  $P(r, \mathbf{x}; t)$  crossing the boundaries of the definition domain of the PDF. Notice that the term in  $J$  takes this form to guarantee that the integration of the PDF in the probabilistic space is always equal to one. In the present case, the domain in the physical space would be the zone of the device upstream from the paper filter, and the “radius” space would be all the (positive) sizes except zero. In fact, the PDF is implicitly conditional on being defined in the described region [20], as we are not interested in particles outside that domain or with meaningless size. No increase or decrease in the size of the particles, including coalescence or breaking up, should be considered, given the low void fraction of particles in diesel. An accumulation is to occur for sure in the paper filter, but this is outside our domain.

In steady-state situations, the last term in Equation (A4) is null, as the same number of particles that enter the definition domain should leave it (either by being trapped in the paper filter or crossing to the other side), so the net flux is zero. In the present case, the PDF transport equation could be considered in a quasi-steady state. The reason is that the effect of the particles on the filter changes very slowly compared to the fluid flow characteristic times, which means that temporal variations of the paper filter properties can be neglected in the transport equation. That is, for the duration of a car ride, changes in the filter properties are negligible.

Should this PDF be described in the Lagrangian frame, it would be represented numerically by particles evolving in the flow in a Monte Carlo simulation. This is essentially what an Eulerian-Lagrangian description does. In the present case, our interest lies in the use of an Eulerian-Eulerian formulation, so the PDF is represented as a set of notional Eulerian fields [7]. Notice that the information obtained is identical for both representations. In fact, in this case, the traditional distinction between Eulerian-Lagrangian and Eulerian-Eulerian is really a distinction between two numerical algorithms to solve what essentially is the same quantity, the PDF of the particle radius (and position).

For the particular situation described in this paper, as the flow is laminar, by using the Eulerian-Eulerian approach, we will end up with non-stochastic Eulerian transport equations for the particle-related magnitudes, whose derivation is the purpose of this appendix. That does not mean that we know exactly the position of every particle in the flow, as the boundary conditions are only known in a probabilistic sense.

From Equations (A2) and (A4), a conservation equation for the number density  $n(r, \mathbf{x}; t)$  is obtained (notice that the last term in Equation (A4) compensates for the one appearing from the time derivative of  $N$  [20]):

$$\begin{aligned} \frac{\partial n(r, \mathbf{x}; t)}{\partial t} = & -\frac{\partial}{\partial x_j} \left[ \overline{\left( \frac{dx_j^+}{dt} \middle| \mathbf{x}, r \right)} n(r, \mathbf{x}; t) \right] \\ & -\frac{\partial}{\partial r} \left[ \overline{\left( \frac{dr^+}{dt} \middle| \mathbf{x}, r \right)} n(r, \mathbf{x}; t) \right] \end{aligned} \quad (\text{A4})$$

In the previous equation, the terms that are conditional on position  $\mathbf{x}$  can be replaced by their Eulerian counterparts:

$$\begin{aligned} \frac{\partial n(r, \mathbf{x}; t)}{\partial t} = & -\frac{\partial}{\partial x_j} \left[ \left( \overline{u^p_j | r} \right) n(r, \mathbf{x}; t) \right] \\ & -\frac{\partial}{\partial r} \left[ \left( \overline{\dot{r} | r} \right) n(r, \mathbf{x}; t) \right] \end{aligned} \quad (\text{A5})$$

In Equation (A6), the variable  $\mathbf{x}$  should be taken in the physical space, no longer in the probabilistic space. The velocity of the particle  $\mathbf{u}^p$  and the radius variation  $\dot{r}$ , as Eulerian quantities, are now functions not only of time but also space.

We have already mentioned that the overline means some kind of ensemble average; for example, we can imagine a set of repeated equivalent systems (filters with diesel and particles). In the case of turbulent flows, as turbulence is a chaotic dynamical system, each individual system will evolve in a different way. In the present case, however, the flow is laminar, which means that the flow is not chaotic, so all the systems would evolve in an identical way. As a consequence, we can safely remove the “overline” from the previous equation. As, in this case, the particles do not change size, Equation (A6), which is particularized for the particles inside the diesel, is rewritten as:

$$\frac{\partial n(r, \mathbf{x}; t)}{\partial t} = -\frac{\partial}{\partial x_j} \left[ u_j^p(r, \mathbf{x}; t) n(r, \mathbf{x}; t) \right] \quad (\text{A6})$$

Once the differential equation for  $n(r, \mathbf{x}; t)$  is set up, the boundary conditions should be prescribed. As the number density is a statistical magnitude, only statistical information is needed. Hence, it is not necessary to prescribe the individual position of each particle, just some kind of PDF information about the boundary.

Now, the second term of the right-hand side of Equation (A1),  $P(\mathbf{v} | r, \mathbf{x}; t)$ , is analyzed. This is the probability density of having a particle velocity value  $v$  conditional on its radius  $r$  and position  $\mathbf{x}$  at time  $t$ . In the present case, being a laminar flow with no particle interaction, this is not a stochastic magnitude: the velocity evolution just depends on those magnitudes under the problem conditions. Its value  $\mathbf{u}^p(r, \mathbf{x}; t)$  is obtained in our problem by solving the transport equation of a small spherical particle in a laminar flow, considering only the dominant, drag, and buoyancy terms [10]:

$$\begin{aligned} (\rho^p + 0.5\rho) \frac{4\pi r^3}{3} \frac{du_i^p}{dt} = & (\rho - \rho^p) \frac{4\pi r^3}{3} g_i \\ & - 3\rho\pi r v (u_i^p - u_i) \\ & - \frac{9\rho\pi r^2}{4} \|u_i^p - u_i\| (u_i^p - u_i) \end{aligned} \quad (\text{A7})$$

where  $\rho^p$  and  $\rho$  are the densities of the particle and the fluid, respectively;  $4\pi r^3/3$  is the volume of a spherical particle with a diameter  $r$ ;  $v$  is the kinematic viscosity;  $\mathbf{u}^p$  is the particle velocity;  $\mathbf{u}$  is the fluid velocity; and  $d/dt$  stands for the total time derivative of the velocity of the particle, that is to say, its total acceleration, or its Lagrangian time derivative. In Equation (A8), the left term represents the linear momentum variation of a spherical particle and its added mass (because of the equivalent volume of fluid, which moves with the particle), whereas, on the right side, there is first a buoyancy contribution and, next, a drag contribution up to the second order to the relative velocities (the velocity of the particle relative to the velocity of the fluid) with an approximation valid for those velocity particles whose Reynolds number, based on the relative velocity, is less than one, or the theoretical observed drag.

Notice that several of these transport equations for the velocity should be solved, once for each radius representative  $r$  considered in the particle size distribution.

At this moment, we have a complete and closed system to calculate all of the variables of interest (before entering the paper filter). To calculate the flux of particles entering the filter, we multiply the velocity particle perpendicular to the filter surface times the particle number for each radius. With this knowledge, the flux of the “volume” or mass of the particles (they do have a constant density) is immediately deduced.

## References

1. Ulbricht, M. Advanced functional polymer membranes. *Polymer* **2006**, *47*, 2217–2262. [[CrossRef](#)]
2. Iliev, O.; Kirsch, R.; Osterroth, S. Combined Depth and Cake Filtration Model Coupled with Flow Simulation for Flat and Pleated Filters. *Chem. Eng. Technol.* **2018**, *41*, 70–78. [[CrossRef](#)]
3. Sun, Y.; Sanaei, P.; Kondic, L.; Cummings, L.J. Modeling and design optimization for pleated membrane filters. *Phys. Rev. Fluids* **2020**, *5*, 044306. [[CrossRef](#)]
4. Von Stockhausen, A.; Mangold, M.P.; Eppinger, D.; Livingston, T. Procedure for determining the allowable particle contamination for diesel fuel injection equipment (FIE). *SAE Int. J. Fuels Lubr.* **2009**, *2*, 294–304. [[CrossRef](#)]
5. Bessee, G.; Hutzler, S. The effects of diesel fuel additives on water separation performance. *SAE Int. J. Fuels Lubr.* **2009**, *2*, 287–293. [[CrossRef](#)]
6. Bensaid, S.; Marchisio, D.L.; Fino, D. Numerical Simulation of soot filtration and combustion within diesel particulate filters. *Chem. Eng. Sci.* **2010**, *65*, 357–363. [[CrossRef](#)]
7. Valiño, L. A field Monte Carlo formulation for calculating the probability density function of a single scalar in a turbulent flow. *Flow Turbul. Combust.* **1998**, *60*, 157–172. [[CrossRef](#)]
8. Valdés-Parada, F.J.; Goyeau, B.; Ochoa-Tapia, J.A. Jump momentum boundary condition at fluid-porous dividing surface: Derivation of the closure problem. *Chem. Eng. Sci.* **2007**, *62*, 4025–4039. [[CrossRef](#)]
9. Pathapati, S.; Sansalone, J.J. CFD Modeling of Particulate Matter Fate and Pressure Drop in a Storm-Water Radial Filter. *J. Environ. Eng.-ASCE* **2009**, *135*, 77–85. [[CrossRef](#)]
10. Loth, E. Numerical approaches for motion of dispersed particles, droplets and bubbles. *Prog. Energy Combust. Sci.* **2000**, *26*, 161–223. [[CrossRef](#)]
11. Ochoa-Tapia, J.; Whitaker, S. Momentum transfer at the boundary between a porous medium and a homogeneous fluid—I. Theoretical development. *Int. J. Heat Mass Transf.* **1995**, *38*, 2635–2646. [[CrossRef](#)]
12. Masarotti, N.; Nithiarasu, P.; Zienkiewicz, O. Natural convection in porous medium-fluid interface problems. A finite element analysis by using the CBS procedure. *Int. J. Numer. Methods Heat Fluid Flow* **2001**, *11*, 473–490. [[CrossRef](#)]
13. Betchen, L.; Straatman, A.; Thompson, B. A nonequilibrium finite-volume model for conjugate fluid/porous/solid domain. *Numer. Heat Transf. A* **2006**, *49*, 543–565. [[CrossRef](#)]
14. Angot, P. Analysis of singular perturbations on the Brinkman problem for fictitious domain models of viscous flows. *Math. Meth. Appl. Sci.* **1999**, *22*, 1395–1412. [[CrossRef](#)]
15. Iliev, O.; Laptev, V. On numerical simulation of flow through oil filters. *Comput. Vis. Sci.* **2004**, *6*, 139–146. [[CrossRef](#)]
16. OpenCFD Ltd. (ESI Group). 2014. Available online: <http://www.openfoam.com> (accessed on 20 December 2022).
17. Jones, M.P.; Storm, M.; York, A.P.E.; Hyde, T.I.; Hatton, G.D.; Greenaway, A.G.; Haigh, S.J.; Eastwood, D.S. 4D In-Situ Microscopy of Aerosol Filtration in a Wall Flow Filter. *Materials* **2020**, *13*, 5676. [[CrossRef](#)] [[PubMed](#)]
18. Williams, F.A. Spray combustion and atomization. *Phys. Fluids* **1992**, *1*, 541. [[CrossRef](#)]
19. Subramaniam, S. Statistical representation of a spray as a point process. *Phys. Fluids* **2000**, *12*, 2413–2431. [[CrossRef](#)]
20. Valiño, L.; Hierro, J. Boundary conditions for probability density function transport equations in fluid mechanics. *Phys. Rev. E* **2003**, *67*, 046310. [[CrossRef](#)] [[PubMed](#)]

**Disclaimer/Publisher’s Note:** The statements, opinions and data contained in all publications are solely those of the individual author(s) and contributor(s) and not of MDPI and/or the editor(s). MDPI and/or the editor(s) disclaim responsibility for any injury to people or property resulting from any ideas, methods, instructions or products referred to in the content.